

1  
2  
3  
4  
5  
6  
7  
8  
9  
10  
11  
12  
13  
14  
15  
16  
17  
18  
19  
20

Supporting Information for

**Towards the development of a national drought monitoring framework for India:  
Reconstruction of historical droughts using CLM5**

Devavat Chiru Naik<sup>1</sup>, Chandrika Thulaseedharan Dhanya<sup>2\*</sup>, Harrie-Jan Hendricks Franssen<sup>3</sup>

<sup>1</sup>Research Scholar, Department of Civil and Environmental Engineering, Indian Institute of Technology Delhi, Hauz Khas, New Delhi, India. email: [Devavat.Chiru.Naik@civil.iitd.ac.in](mailto:Devavat.Chiru.Naik@civil.iitd.ac.in)

<sup>2</sup>Professor, Department of Civil and Environmental Engineering, Indian Institute of Technology Delhi, Hauz Khas, New Delhi, India. email: [dhanya@civil.iitd.ac.in](mailto:dhanya@civil.iitd.ac.in)

<sup>3</sup>Professor, Agrosphere (IBG-3), Forschungszentrum Juelich GmbH, Juelich, Germany. email: [h.hendricks-franssen@fz-juelich.de](mailto:h.hendricks-franssen@fz-juelich.de)

**\*Corresponding author:**

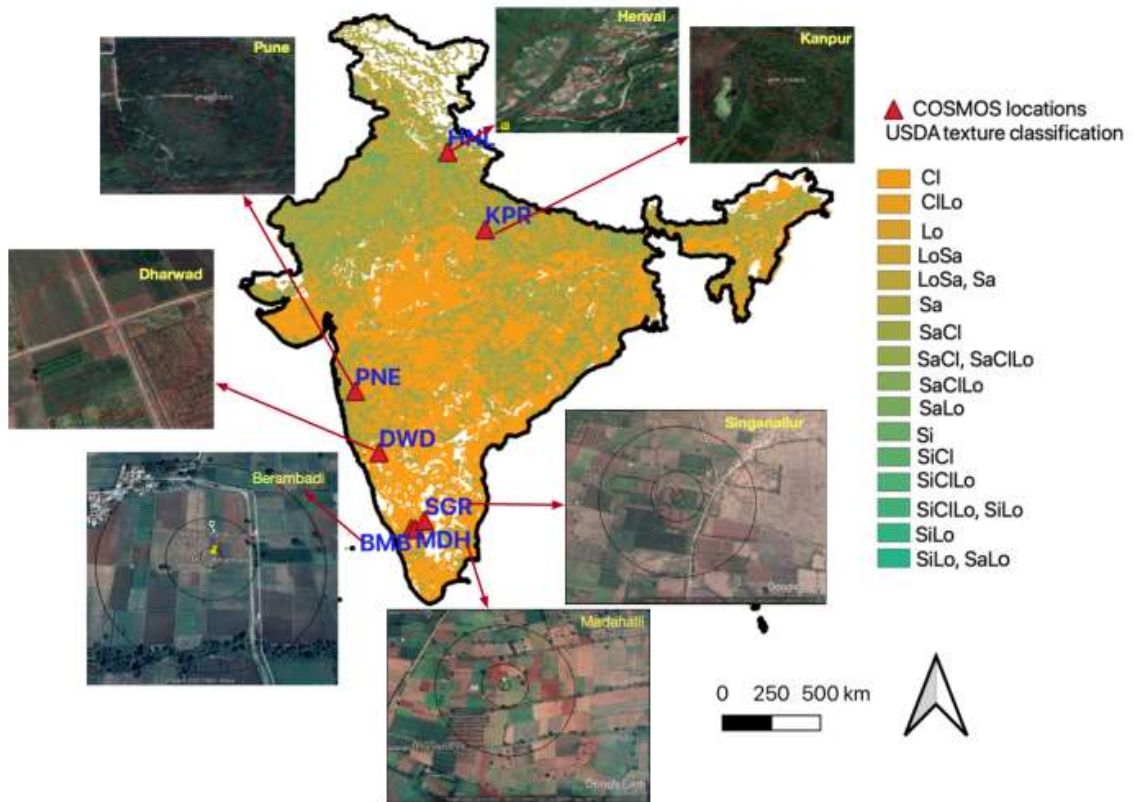
Chandrika Thulaseedharan Dhanya, Professor, Department of Civil and Environmental Engineering, Indian Institute of Technology Delhi, New Delhi-110016, India; Email: [dhanya@civil.iitd.ac.in](mailto:dhanya@civil.iitd.ac.in); Office Phone Number: +91-11-26597328.

**Content of this file**

**Fig. S1 to S26**

**Tables S1 to S6**

## Indian COSMOS network (ICON) over India soil map



21

22 **Figure S1.** Locations of the Indian COSMOS Network (ICON) sites. The base map displays the soil  
 23 texture of India (Source: NRSC), where Cl = Clay, Lo = Loam, Sa = Sand, and Si = Silt. The inset  
 24 photos show the precise location of each site on Google Earth imagery, indicating the 50 m and 200  
 25 m impact areas. Figure adapted from Updhaya et al. (2021).

26

27

28

29

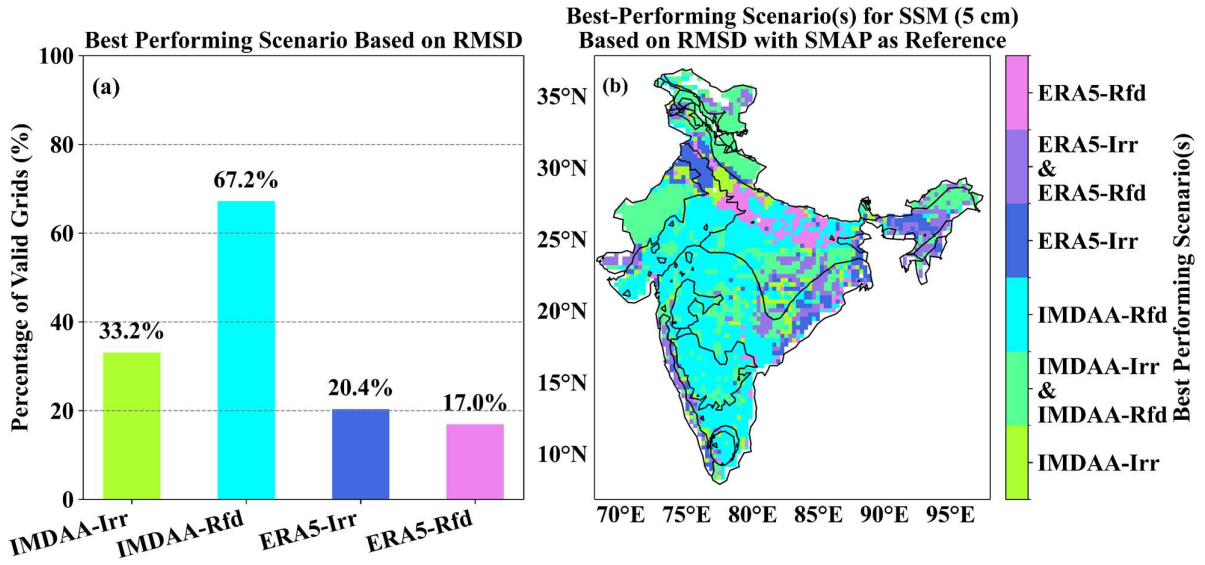
30

31

32

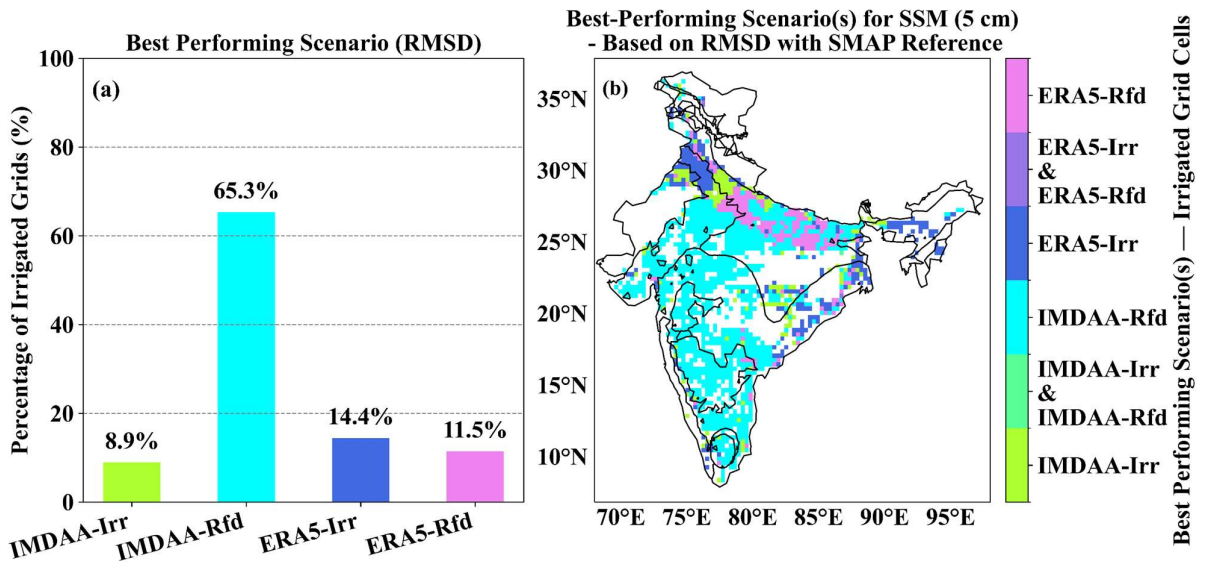
33

34



35

36 **Figure S2:** (a) Percentage of grid cells where each CLM5 simulations of surface soil moisture (5 cm)  
 37 achieves the lowest RMSD relative to SMAP. (b) Spatial distribution of the best-performing  
 38 simulation across grid cells.

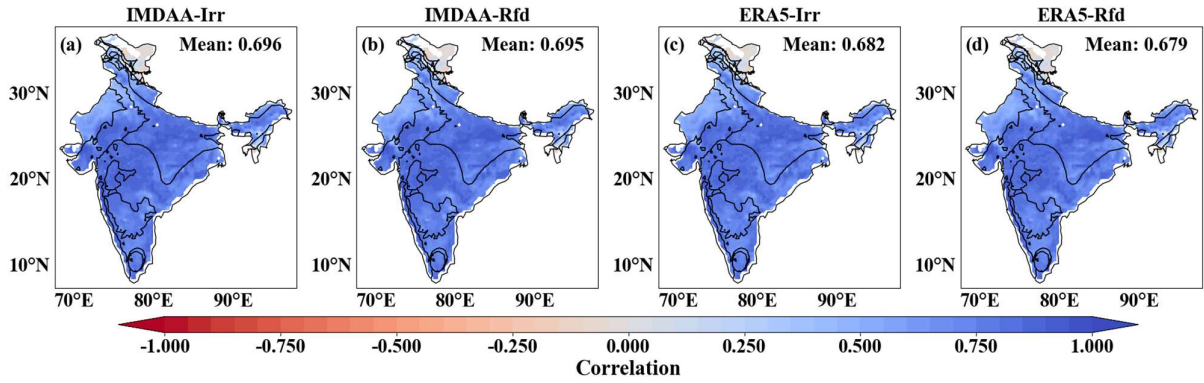


39

40 **Figure S3:** (a) Percentage of irrigated grid cells where each CLM5 simulations of soil moisture at 5  
 41 cm depth shows the lowest RMSD relative to SMAP. (b) Spatial distribution of the best-performing  
 42 simulation across irrigated grid cells.

43

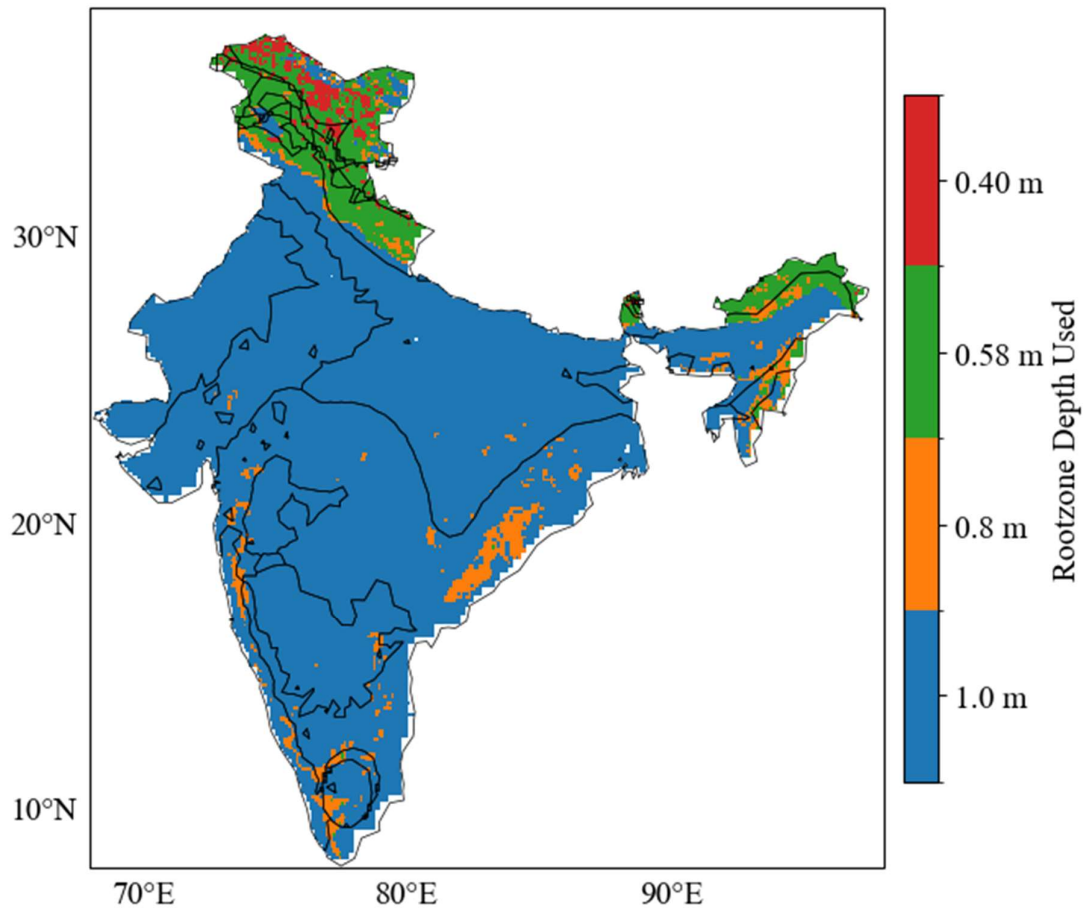
44



45

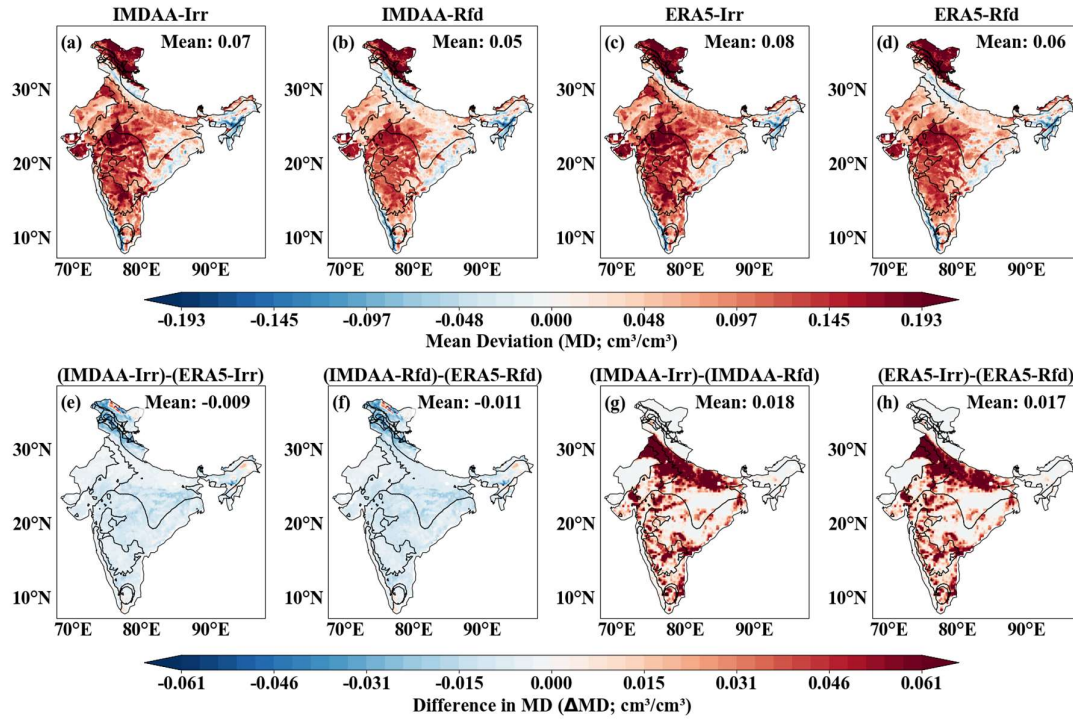
46 **Figure S4:** Grid-wise spatial distribution of Spearman correlation coefficients between CLM5-  
 47 simulated surface soil moisture (SSM, 5 cm) and SMAP observations across India. Panels (a–d)  
 48 correspond to IMDAA-Irr, IMDAA-Rfd, ERA5-Irr, and ERA5-Rfd, respectively.

49



50

51 **Figure S5.** Spatial distribution of rootzone soil moisture (RZSM) depths used in the analysis, adjusted  
 52 for bedrock depth across India. Color codes represent the effective rootzone depths applied at each  
 53 grid cell: 0.40 m (red), 0.58 m (green), 0.80 m (orange), and 1.00 m (blue), based on local soil and  
 54 bedrock constraints.



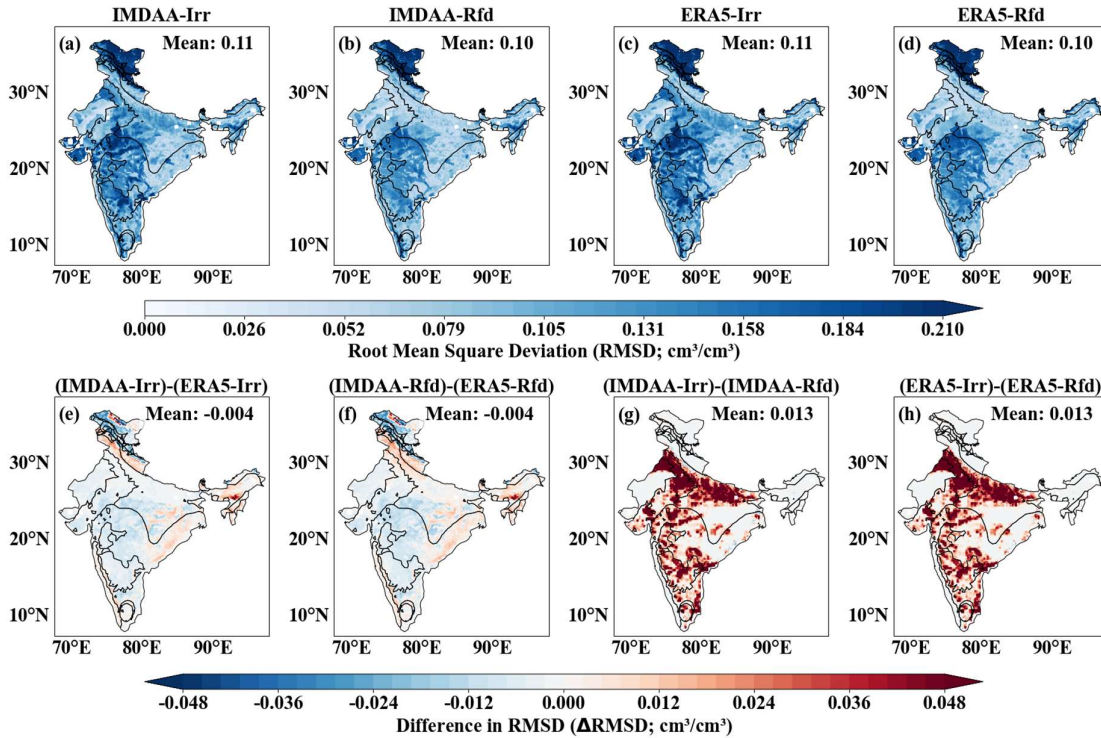
55

56 **Figure S6:** Grid-wise Mean Deviation (MD) of SSM (10 cm) simulated by CLM5 relative to  
 57 GLEAM across India for 1980–2020. Panels (a–d) show MD for IMDAA-Irr, IMDAA-Rfd, ERA5-  
 58 Irr, and ERA5-Rfd. Panels (e–f) present differences in MD ( $\Delta$ MD) highlighting the influence of  
 59 atmospheric forcing (IMDAA vs. ERA5), while panels (g–h) illustrate the impact of irrigation by  
 60 contrasting irrigated and rainfed configurations.

61

62 Figure S6 presents the grid-wise Mean Deviation (MD) patterns of CLM5-simulated surface soil  
 63 moisture (SSM, 10 cm) relative to GLEAM. The spatial bias structure closely resembles the SMAP-  
 64 based assessment, with widespread wet biases across northwest, central, peninsular, and parts of  
 65 northern and northeastern India, and negative biases along the eastern and western coasts and portions  
 66 of northeastern India. Rainfed simulations generally exhibit smaller biases, whereas irrigated  
 67 configurations reinforce wet biases across irrigated regions (Figure S6g–h). Among the experiments,  
 68 IMDAA-driven runs show the lowest overall MD (Figure S6e–f), indicating improved bias  
 69 representation relative to ERA5-driven simulations.

70



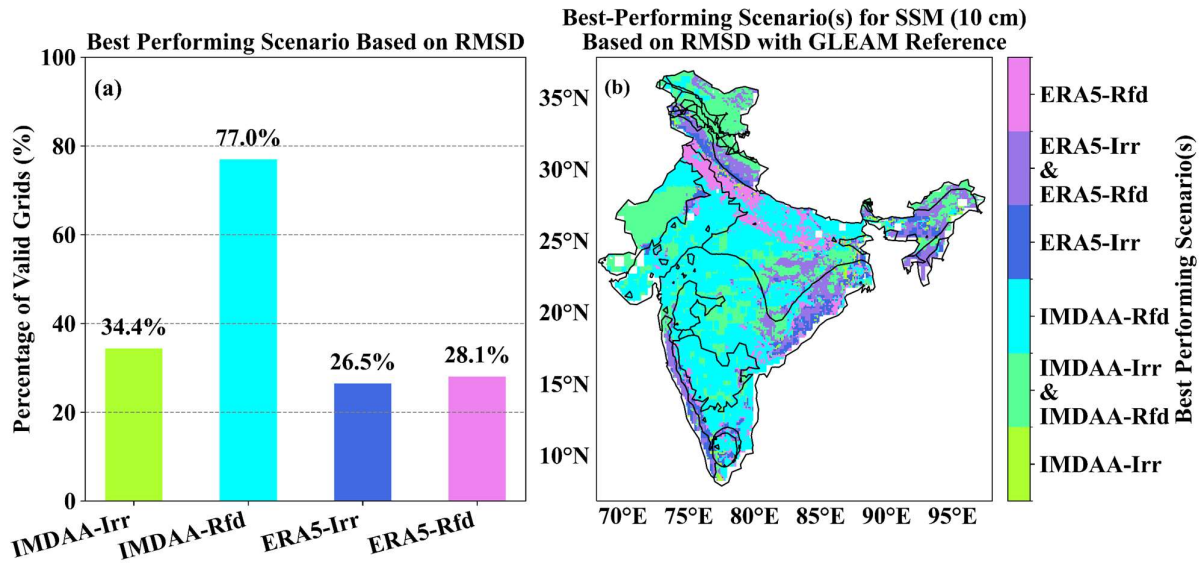
71

72 **Figure S7:** Grid-wise Root Mean Square Deviation (RMSD) of SM (10 cm) simulated by CLM5  
 73 relative to GLEAM across India for 1980–2020. Panels (a–d) show RMSD for IMDAA-Irr, IMDAA-  
 74 Rfd, ERA5-Irr, and ERA5-Rfd. Panels (e–f) present differences in RMSD ( $\Delta$ RMSD) highlighting the  
 75 influence of atmospheric forcing (IMDAA vs. ERA5), while panels (g–h) illustrate the impact of  
 76 irrigation by contrasting irrigated and rainfed configurations.

77

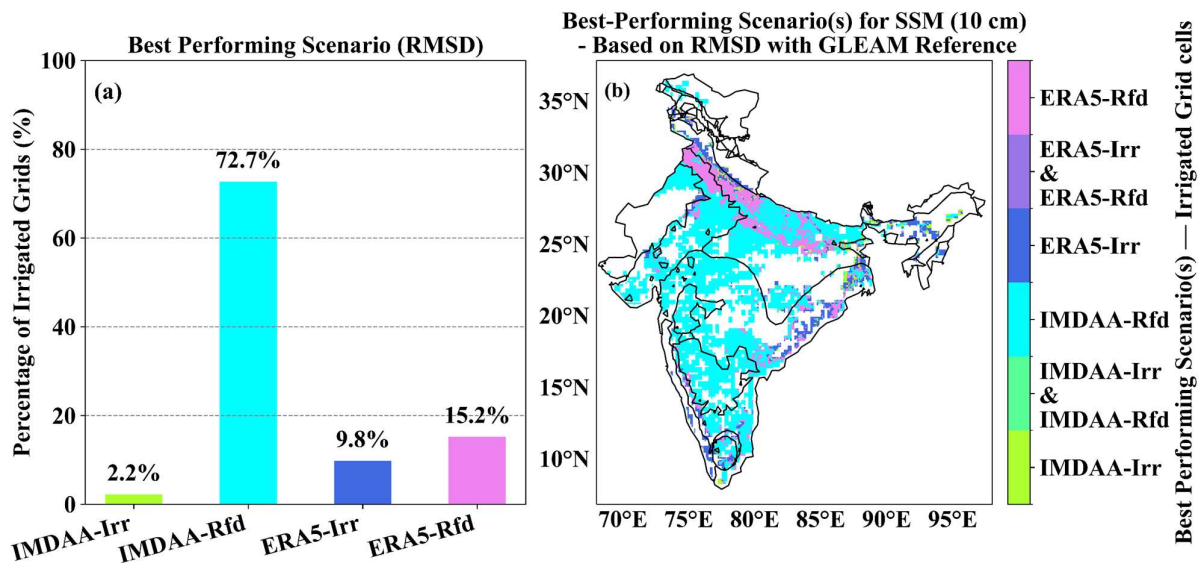
78 Figure S7 presents the grid-wise Root Mean Square Deviation (RMSD) of CLM5-simulated surface  
 79 soil moisture relative to GLEAM. Mean RMSD is slightly lower for rainfed configurations (IMDAA-  
 80 Rfd: 0.10; ERA5-Rfd: 0.10) than for irrigated runs (IMDAA-Irr: 0.11; ERA5-Irr: 0.11), indicating  
 81 improved performance under rainfed conditions, consistent with the SMAP-based evaluation. Higher  
 82 RMSD values ( $>0.11 \text{ cm}^3 \text{ cm}^{-3}$ ) persist across northeastern, central, southern, and northern regions,  
 83 with errors generally more pronounced in irrigated simulations. The  $\Delta$ RMSD patterns (Figure S7e–  
 84 h) further mirror the SMAP results, with IMDAA-driven runs exhibiting lower RMSD across large  
 85 parts of central and southern India, portions of northwestern India, and localized northern regions  
 86 ( $\Delta$ RMSD  $\approx -0.004 \text{ cm}^3 \text{ cm}^{-3}$ ), whereas ERA5-driven simulations perform better along the  
 87 southeastern coast, northeastern India, and parts of the Indo-Gangetic Plain. These patterns are  
 88 quantified in Supplementary Figure S8, where IMDAA-Rfd achieves the lowest RMSD at 77% of  
 89 grid cells. Over irrigated regions, higher RMSD dominates most grid cells (Figure S7g–h), although  
 90 IMDAA-Rfd still performs best at 77.2% of irrigated locations, particularly across central and

91 peninsular India (Figure S9). As in the SMAP comparison, rainfed simulations outperform irrigated  
 92 configurations across much of the Indo-Gangetic Plain. Correlation maps (Figure S19) show strong  
 93 temporal agreement between CLM5 simulations and GLEAM across most of India ( $\rho > 0.8$ ), further  
 94 supporting the robustness of the SMAP-based performance assessment.



95

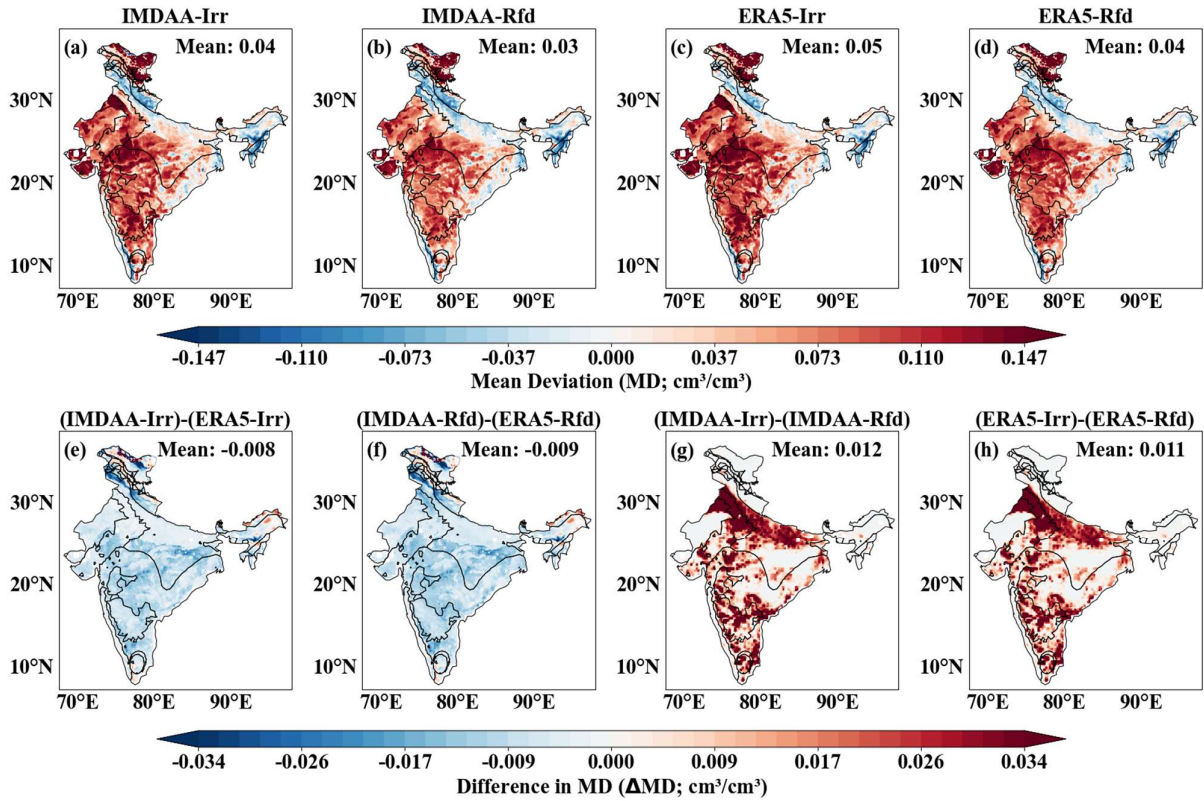
96 **Figure S8:** (a) Percentage of grid cells where each CLM5 simulations of surface soil moisture (SSM,  
 97 10 cm) achieves the lowest RMSD relative to GLEAM. (b) Spatial distribution of the best-performing  
 98 simulation across grid cells.



99

100 **Figure S9.** (a) Percentage of irrigated grid cells where each CLM5 simulations of soil moisture  
 101 (SSM) at 10 cm depth shows the lowest RMSD relative to GLEAM. (b) Spatial distribution of the  
 102 best-performing simulation across irrigated grid cells.

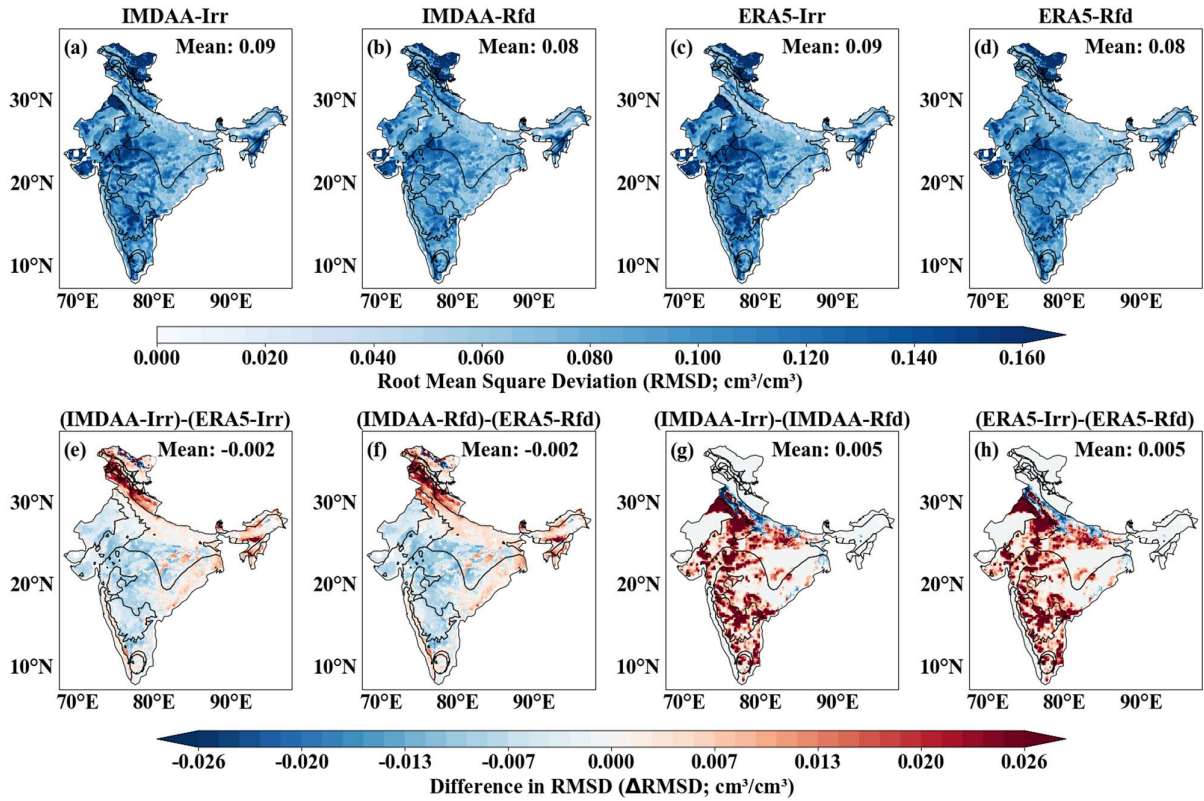
103



104

105 **Figure S10:** Grid-wise Mean Deviation (MD) of RZSM (100 cm) simulated by CLM5 relative to  
 106 GLEAM across India for 1980–2020. Panels (a–d) show MD for IMDAA-Irr, IMDAA-Rfd, ERA5-  
 107 Irr, and ERA5-Rfd. Panels (e–f) present differences in MD ( $\Delta$ MD) highlighting the influence of  
 108 atmospheric forcing (IMDAA vs. ERA5), while panels (g–h) illustrate the impact of irrigation by  
 109 contrasting irrigated and rainfed configurations.

110

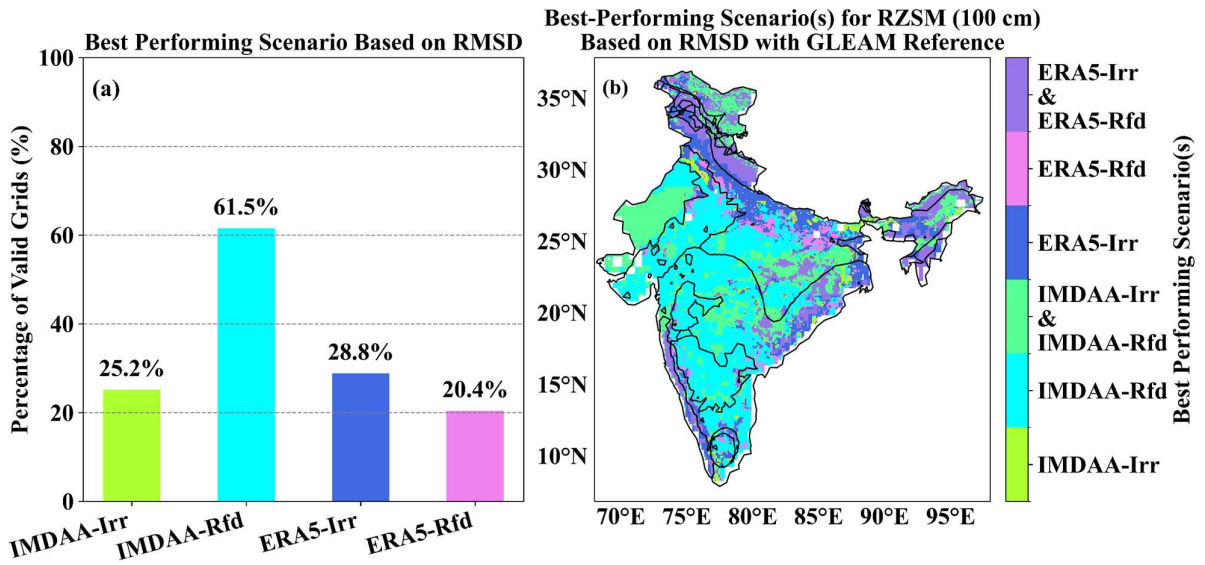


111

112 **Figure S11:** Grid-wise Root Mean Square Deviation (RMSD) of RZSM (100 cm) simulated by  
 113 CLM5 relative to GLEAM across India for 1980–2020. Panels (a–d) show RMSD for IMDAA-Irr,  
 114 IMDAA-Rfd, ERA5-Irr, and ERA5-Rfd. Panels (e–f) present differences in RMSD ( $\Delta$ RMSD)  
 115 highlighting the influence of atmospheric forcing (IMDAA vs. ERA5), while panels (g–h) illustrate  
 116 the impact of irrigation by contrasting irrigated and rainfed configurations.

117

118

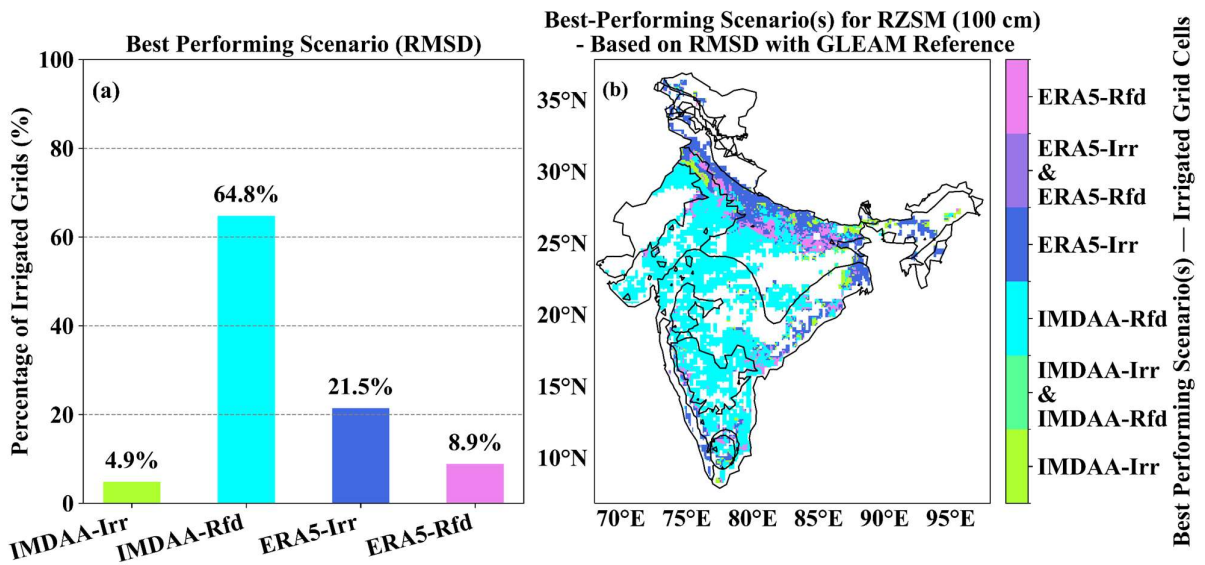


119

120 **Figure S12:** (a) Percentage of grid cells where each CLM5 simulations of RZSM (100 cm) achieves  
 121 the lowest RMSD relative to GLEAM. (b) Spatial distribution of the best-performing simulation  
 122 across grid cells.

123

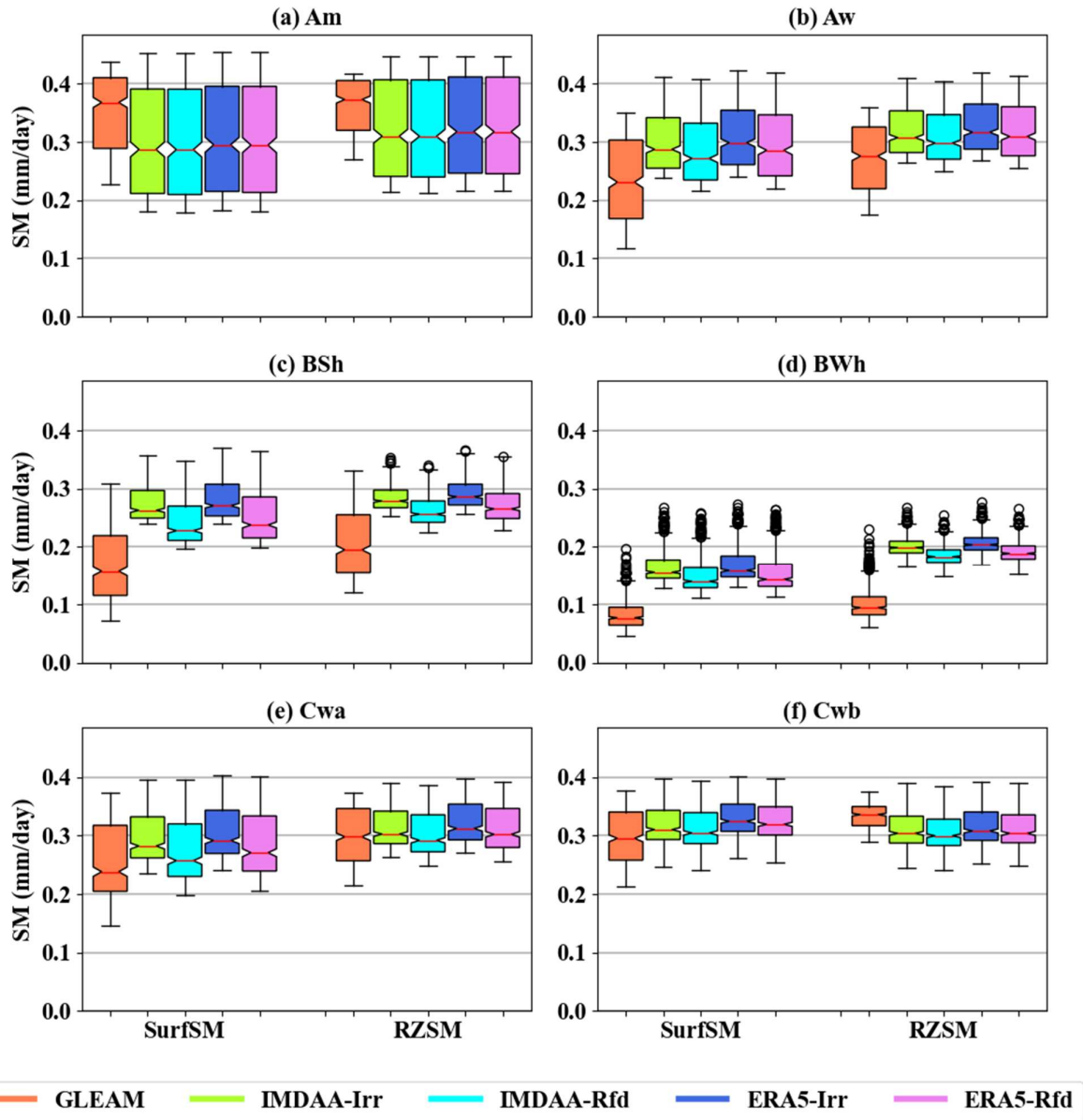
124



125

126 **Figure S13.** (a) Percentage of irrigated grid cells where each CLM5 simulations of RZSM (100 cm)  
 127 shows the lowest RMSD relative to GLEAM. (b) Spatial distribution of the best-performing  
 128 simulation across irrigated grid cells.

129



130

131 **Figure S14:** Comparison of CLM5SP-simulated soil moisture with GLEAM observations across six  
 132 climate zones. Panels (a–f) show boxplots over Am, Aw, BSh, BWh, Cwa, and Cwb zones. In the  
 133 boxplots, the line inside each box indicates the median, the box spans the interquartile range (25th–  
 134 75th percentile), whiskers extend to  $1.5 \times \text{IQR}$ , and outliers are shown as circles.

135

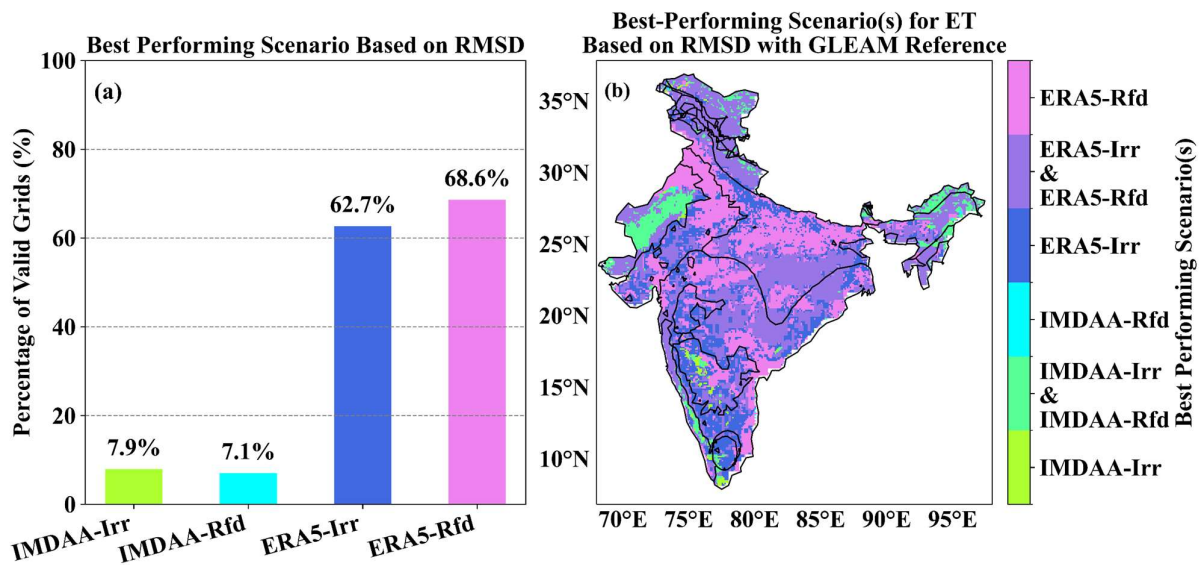
136 A climate zone–wise evaluation of CLM5-simulated soil moisture at 10 cm (SSM) and 100 cm  
 137 (RZSM) depths against GLEAM is presented in Figure S14 and Tables S3–S4. RMSE values range  
 138 from  $0.03\text{--}0.12 \text{ m}^3 \text{ m}^{-3}$  for SSM and  $0.02\text{--}0.11 \text{ m}^3 \text{ m}^{-3}$  for RZSM, with the lowest errors consistently  
 139 observed in the humid subtropical zones (Cwa and Cwb). IMDAA-Rfd generally shows the best  
 140 performance across climate zones; however, at Am for SSM all simulations perform similarly, while

141 for RZSM ERA5-based simulations in Am and both ERA5 and IMDAA-Irr in Cwb exhibit  
142 comparable or improved performance.

143 For SSM, mean deviation (MD) is predominantly positive ( $0.02\text{--}0.12\text{ m}^3\text{ m}^{-3}$ ), with the largest  
144 wet biases occurring in semi-arid and arid regions (BSh and BWh), whereas the Am zone shows a  
145 notable dry bias. Rainfed simulations (IMDAA-Rfd and ERA5-Rfd) generally yield lower biases than  
146 irrigated runs, except in the Am zone for SSM.

147 Spearman correlation coefficients range from 0.76–0.97 for SSM, indicating strong temporal  
148 agreement overall. Lower correlations are observed in the BWh and Cwb zones, particularly for  
149 RZSM.

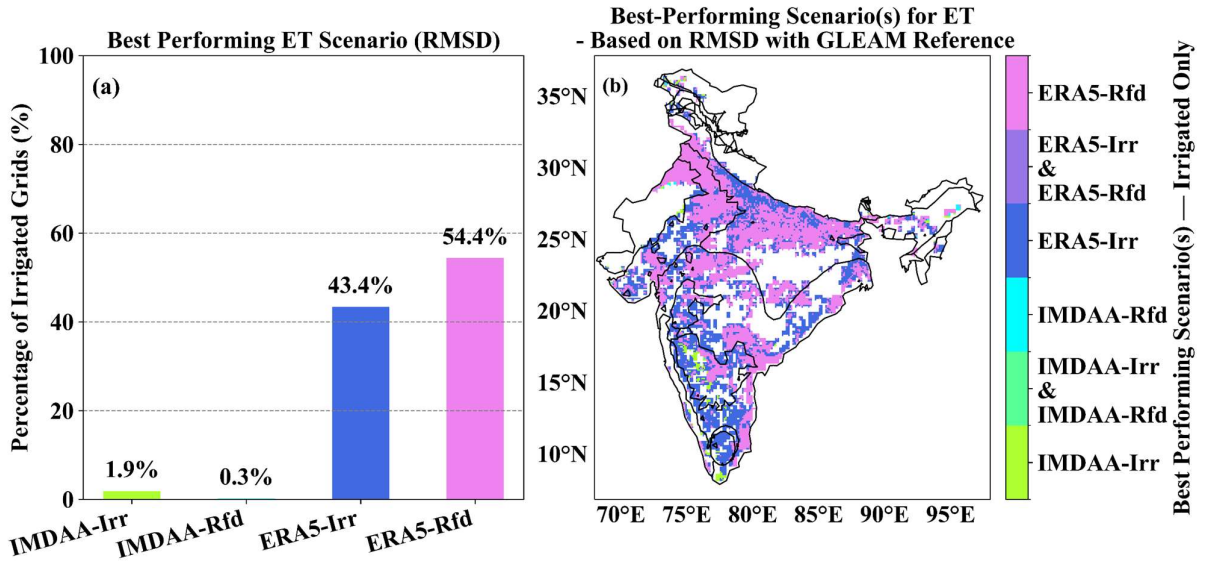
150



151

152 **Figure S15:** (a) Percentage of grid cells where each CLM5 simulations of ET achieves the lowest  
153 RMSD relative to GLEAM. (b) Spatial distribution of the best-performing simulation across grid  
154 cells.

155



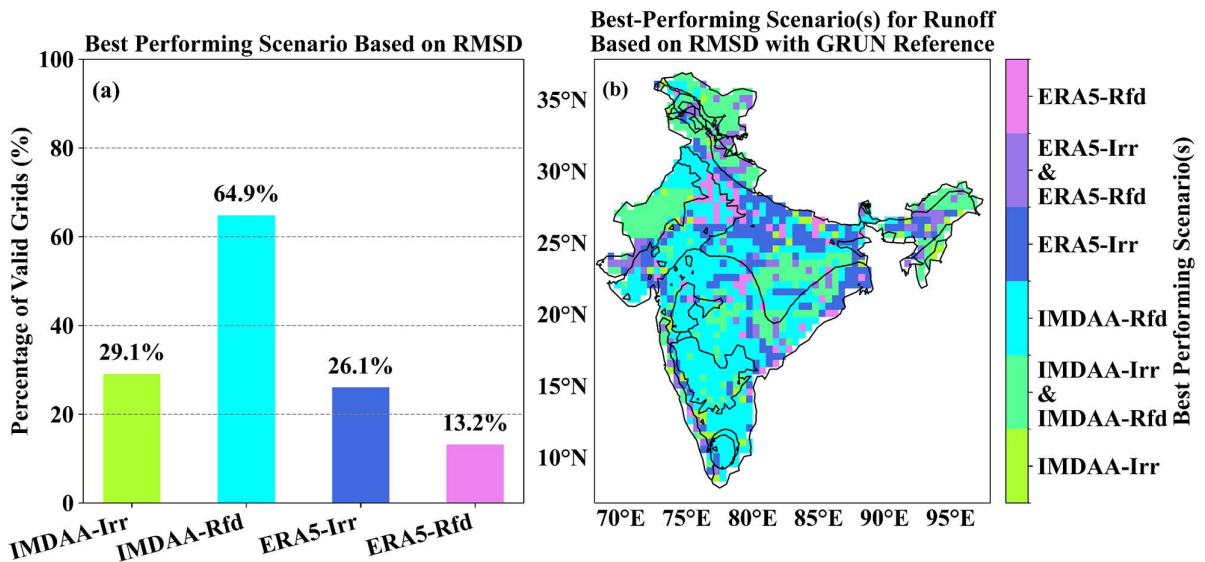
156

157 **Figure S16.** (a) Percentage of irrigated grid cells where each CLM5 simulations of ET shows the  
 158 lowest RMSD relative to GLEAM. (b) Spatial distribution of the best-performing simulation across  
 159 irrigated grid cells.

160

161

162

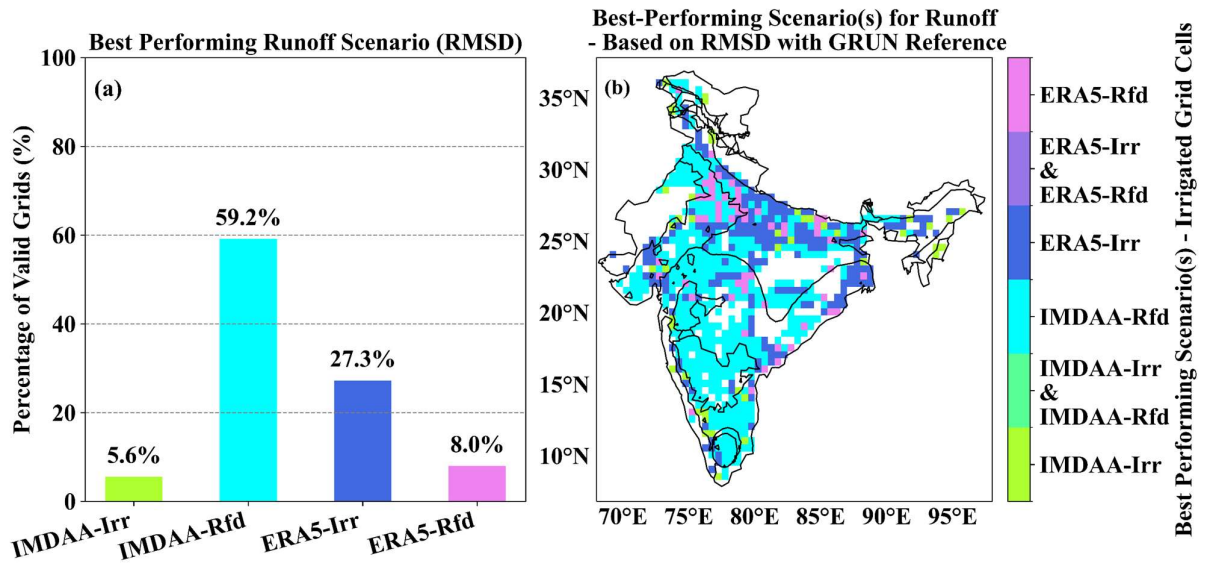


163

164 **Figure S17:** (a) Percentage of grid cells where each CLM5 simulations of Runoff achieves the lowest  
 165 RMSD relative to GLEAM. (b) Spatial distribution of the best-performing simulation across grid  
 166 cells.

167

168



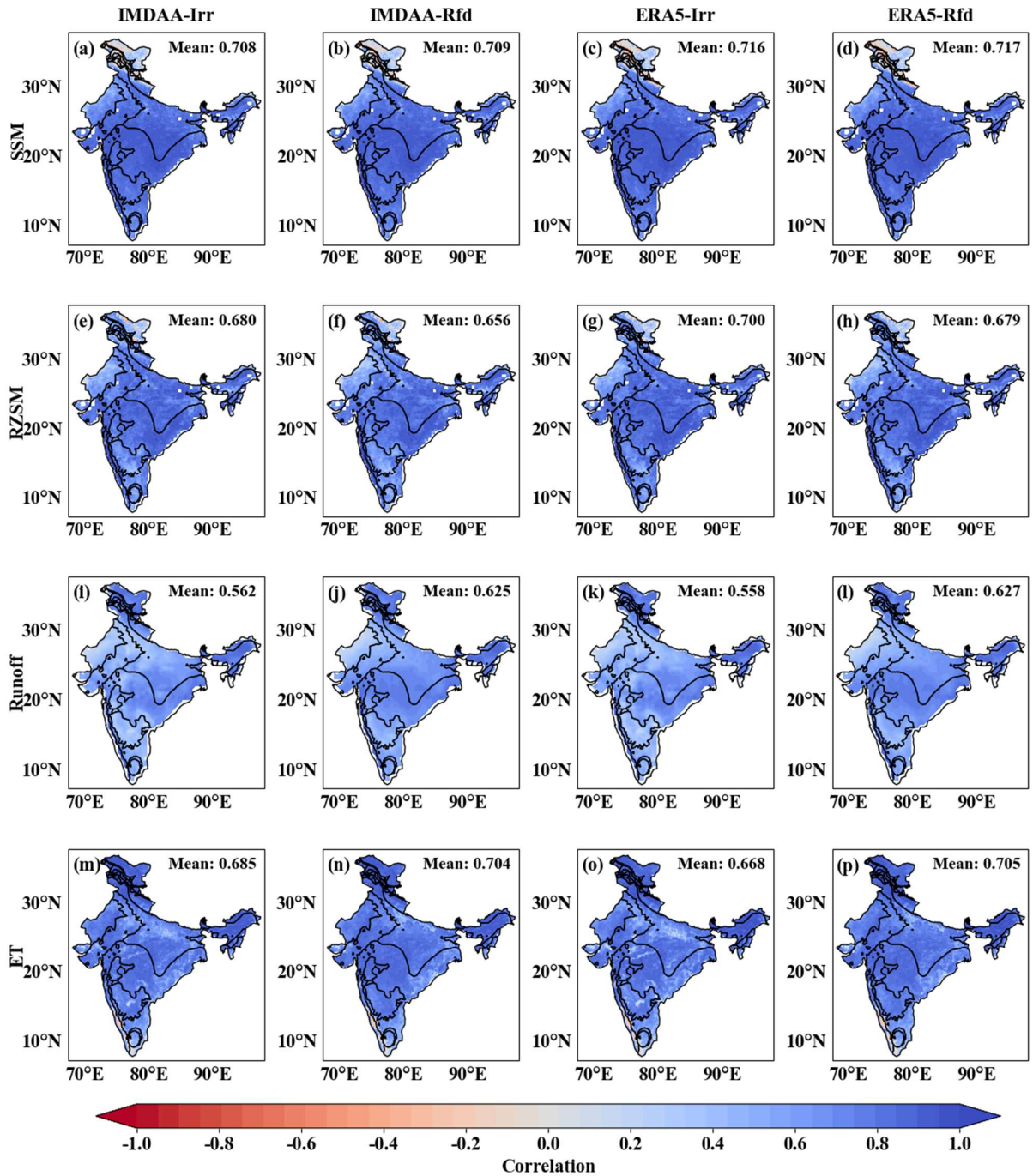
169

170 **Figure S18.** (a) Percentage of irrigated grid cells where each CLM5 simulations of Runoff shows the  
 171 lowest RMSD relative to GLEAM. (b) Spatial distribution of the best-performing simulation across  
 172 irrigated grid cells.

173

174

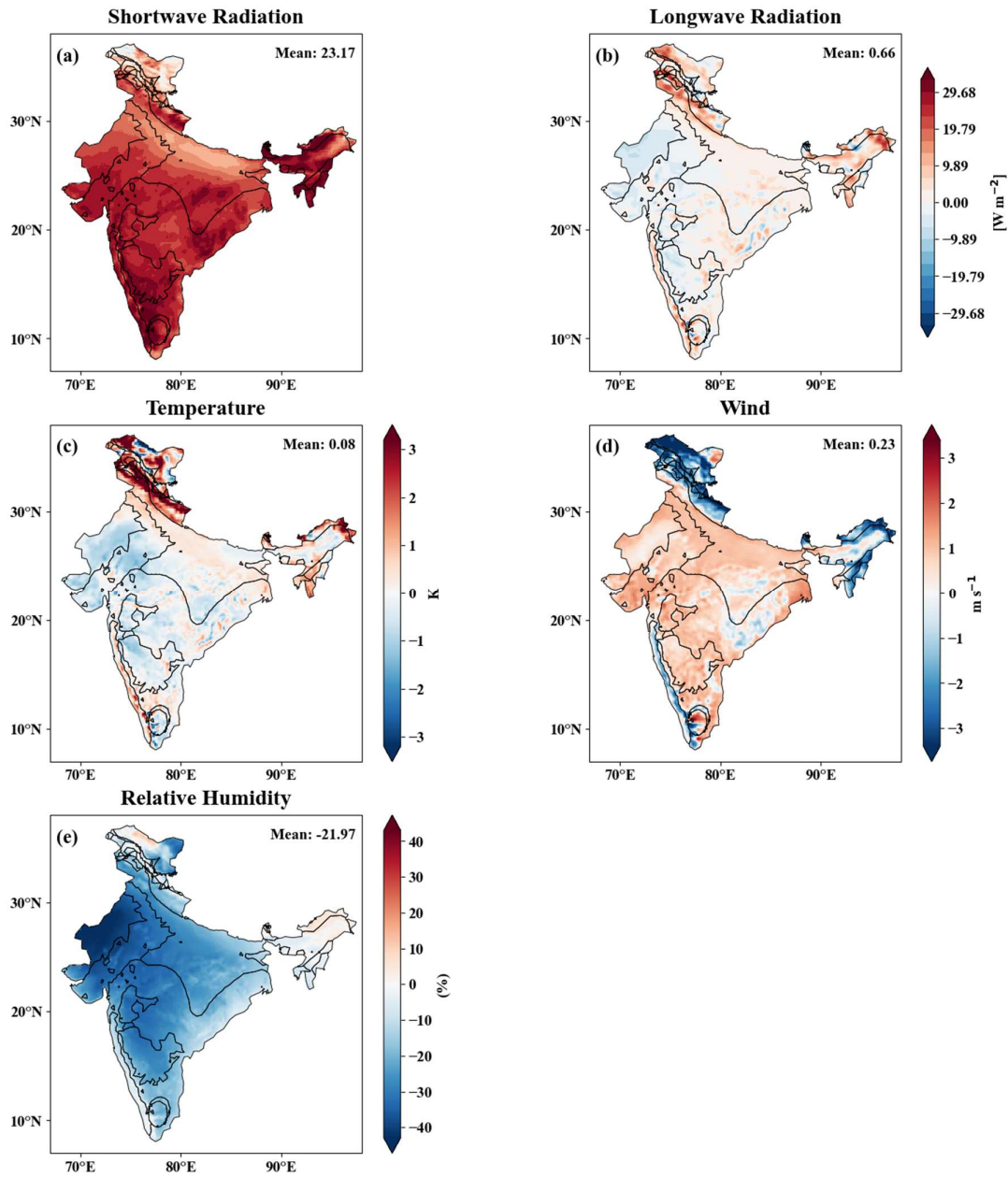
175



176

177 **Figure S19:** Grid-wise Spearman-Correlation analysis of CLM5 simulations against GLEAM SSM,  
 178 RZSM, ET, and GRUN Runoff across India.

179

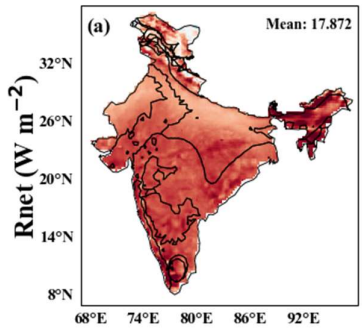


180

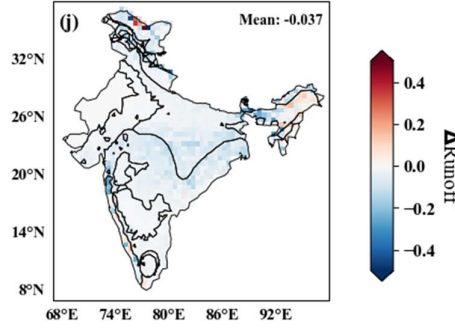
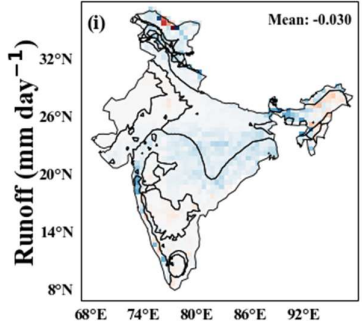
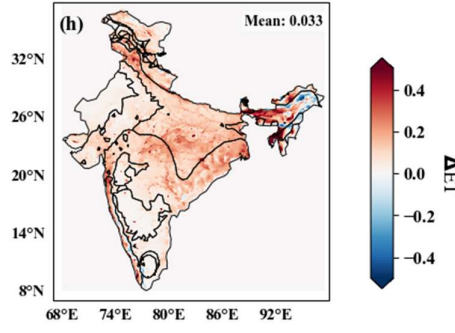
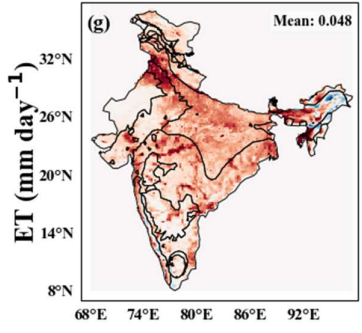
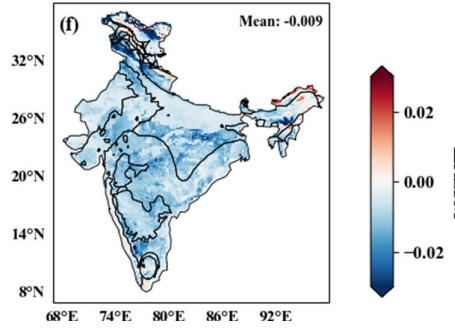
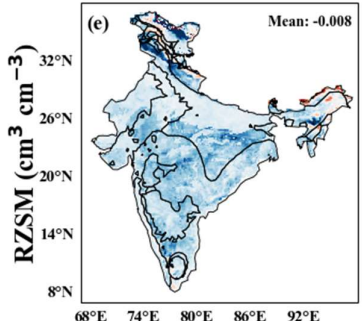
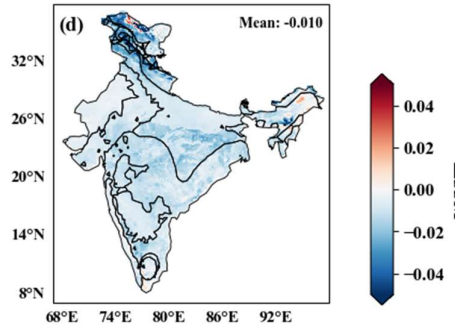
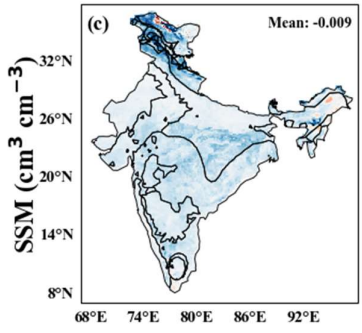
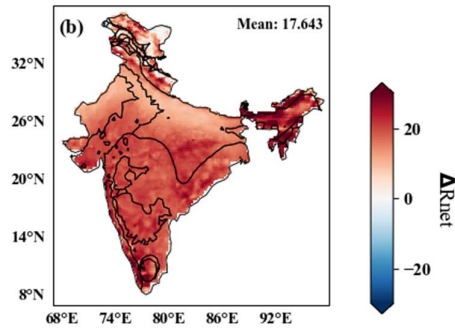
181 **Figure S20.** shows the spatial distribution of the differences between IMDAA and ERA5 forcings of  
 182 Panels (a) Shortwave radiation, (b) Longwave radiation, (c) Temperature at 2m, (d) Wind, and (e)  
 183 Relative humidity.

184

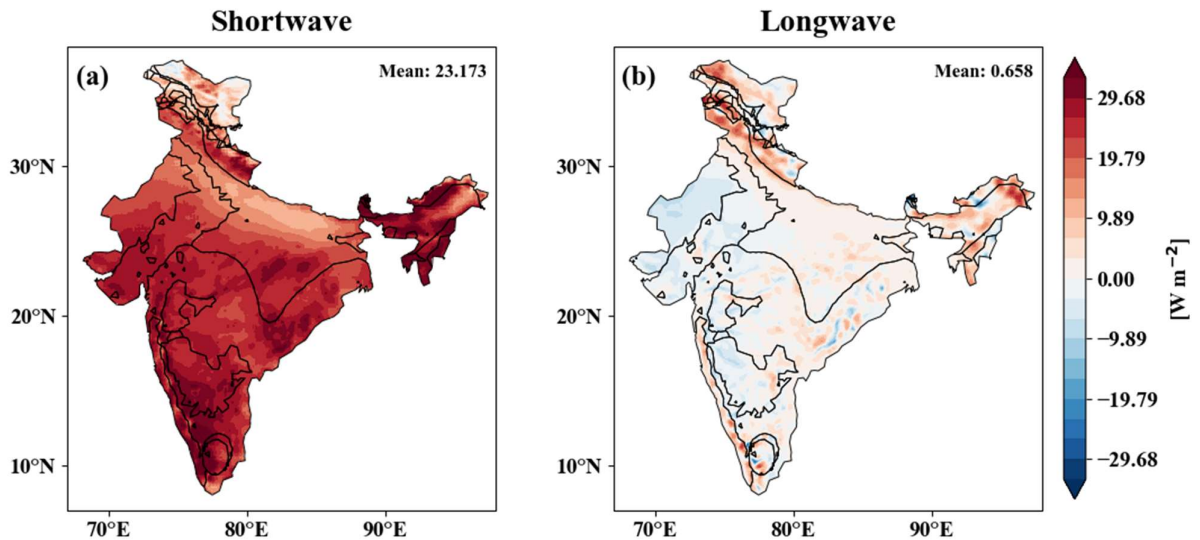
(a) IMDAA-Irr – ERA5-Irr



(b) IMDAA-Rfd – ERA5-Rfd

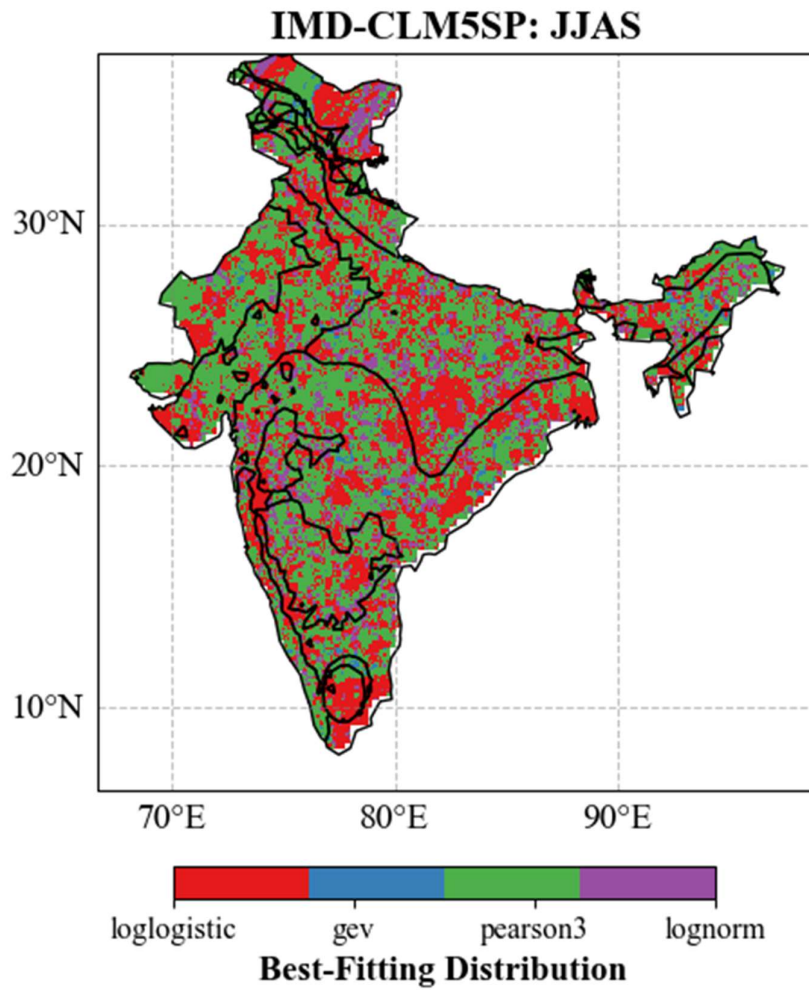


186 **Figure S21.** shows the spatial distribution of the irrigation-induced differences in various variables  
 187 over India for the period 1980–2020. The differences were calculated by subtracting rainfed from  
 188 irrigated simulations. Panels (a) and (b) represent the Rnet differences, while (c) and (d) show the  
 189 differences for SSM. Panels (e) and (f) correspond to RZSM, and (g) and (h) show the differences in  
 190 ET. Lastly, runoff differences are presented in panels (i) and (j). Panels with odd letters (a, c, e, g, i)  
 191 display the differences derived from IMDAA atmospheric forcing (IMDAA-Irr – IMDAA-Rfd),  
 192 whereas panels with even letters (b, d, f, h, j) are for the ERA5 forcing (ERA5-Irr – ERA5-Rfd).  
 193



194

195 **Figure S22.** Spatial distribution of the difference in (a) Shortwave Radiation and (b) Longwave  
 196 Radiation between the IMDAA and ERA5 atmospheric forcings.



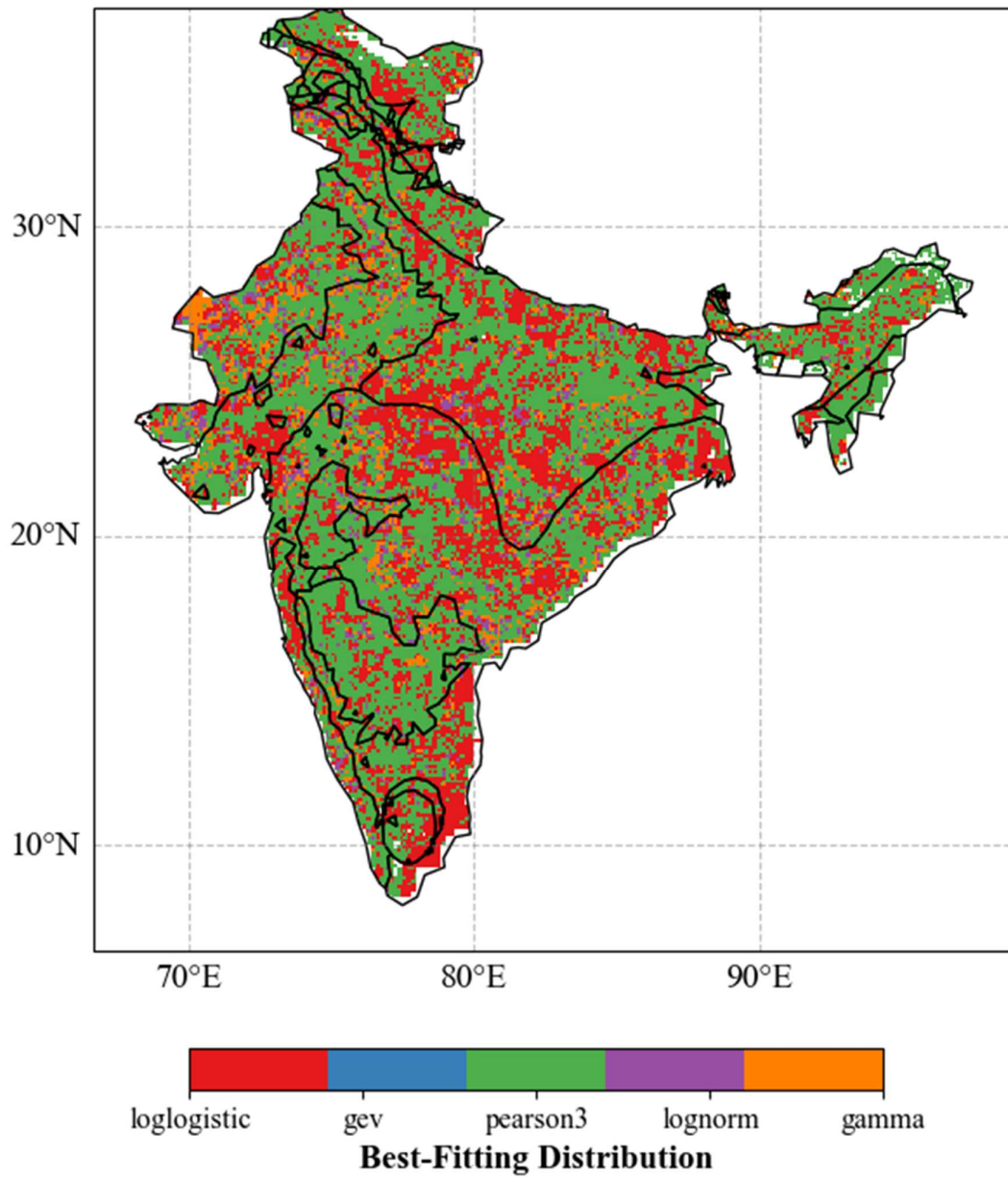
197

198

199 **Figure S23:** Best-Fitted Distribution of Net Precipitation (P-PET) Monsoon (JJAS:sum) data

200

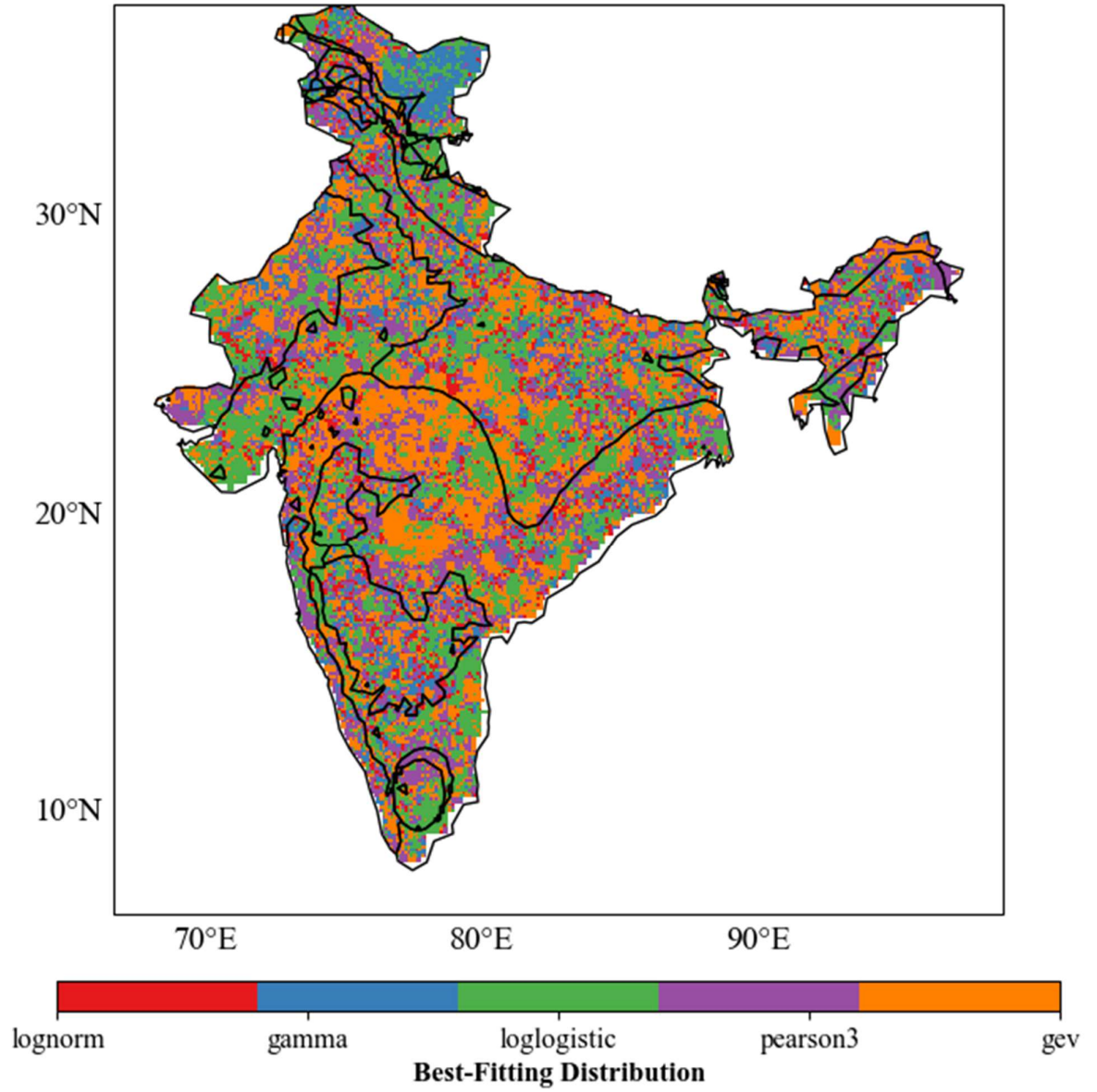
CLM5SP: JJAS



201

202 **Figure S24:** Best-Fitted Distribution of soil moisture Monsoon (JJAS:sum) data

203



204  
 205  
 206

**Figure S25:** Best-Fitted Distribution of CLM5SP runoff Water year (June-May:sum) data

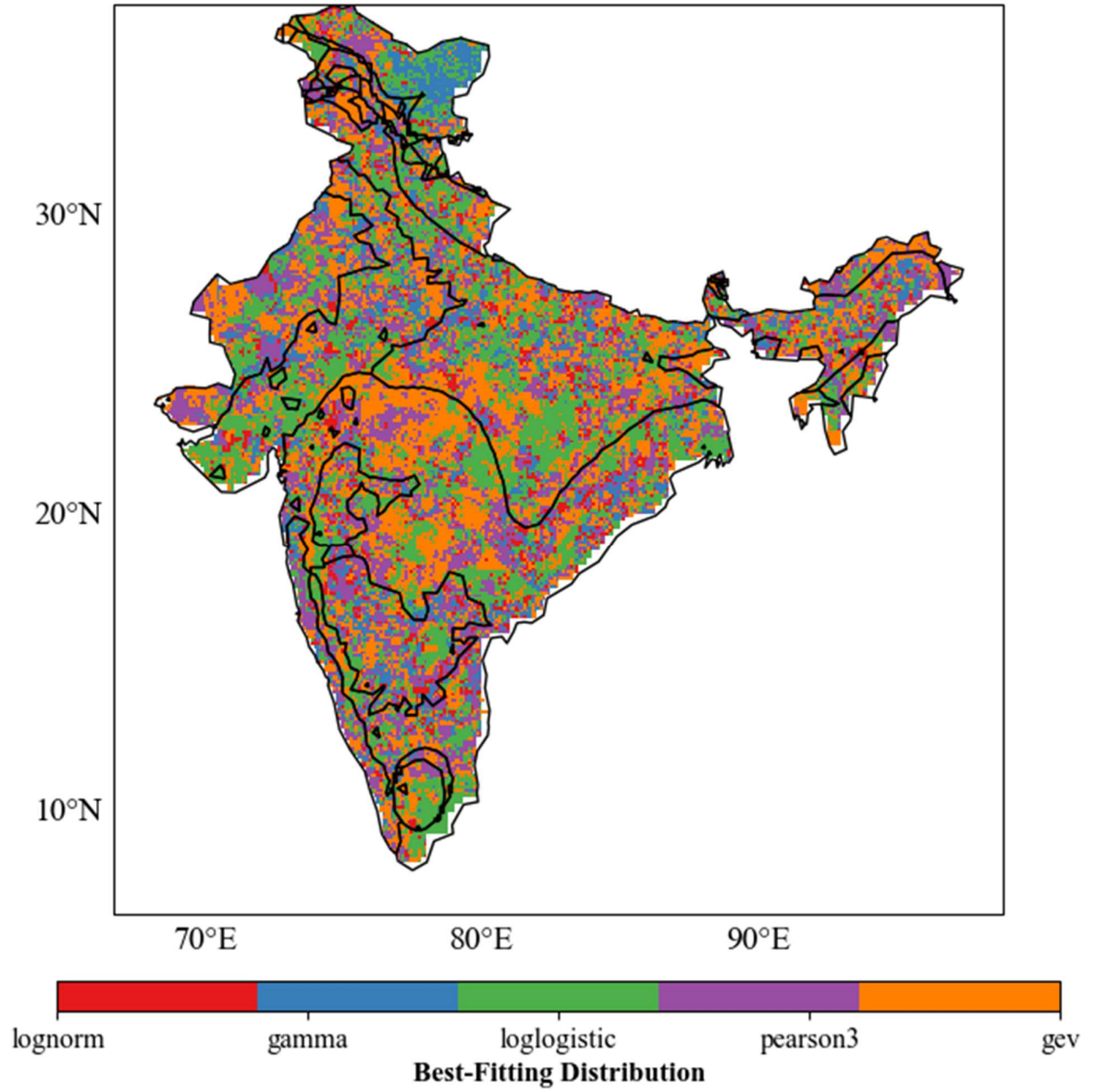


**Figure S26:** Best-Fitted Distribution of CLM5SP runoff monsoon (June-Sep:sum) data

207  
 208  
 209  
 210  
 211  
 212  
 213  
 214  
 215

216 **Table S1: Details of the in-situ soil moisture (COSMOS sensors) stations used in this**  
 217 **study.**

218 More details can be found in (Upadhyaya et al., 2021).

219

S. No	Acronym	Latitude	Longitude	City, State	Data availability	Number of Observations
1	BMB	11.76 <sup>0</sup>	76.58 <sup>0</sup>	Berambadi, Karnataka	20-Sep-2015 to 19-Dec-2019	490
2	MDH	11.73 <sup>0</sup>	76.78 <sup>0</sup>	Madahalli, Karnataka	05-Feb-2016 to 19-Dec-2019	1193
3	SGR	12.14 <sup>0</sup>	77.22 <sup>0</sup>	Singanallur, Karnataka	9-Jun-2015 to 19-Dec-2019	1513

220

221

222 **Table S2: Distribution of selected rootzone soil moisture depths used across 28,941 grid points**

S. No	Depth (m)	Grid Count	Share of Total (%)	23
				224
1	1.00	23,716	81.946	225
2	0.80	1467	5.068	226
3	0.50	2814	9.723	227
4	0.40	494	1.706	228
<b>Total Grid points</b>			<b>28,941</b>	229

230

231

232

233

234

235

236

237

238

**Table S3:** Performance metrics (RMSE, ME, and  $\rho$ ) for soil moisture vs GLEAM (SM: 10 cm).

<b>Climate Zone</b>	<b>Metric</b>	<b>IMDAA-Irr</b>	<b>IMDAA-Rfd</b>	<b>ERA5-Irr</b>	<b>ERA5-Rfd</b>
<b>Am</b>	MD (cm <sup>3</sup> /cm <sup>3</sup> )	-0.05	-0.05	-0.05	-0.05
	RMSD (cm <sup>3</sup> /cm <sup>3</sup> )	0.06	0.06	0.06	0.06
	$\rho$	0.97	0.97	0.97	0.97
<b>Aw</b>	MD (cm <sup>3</sup> /cm <sup>3</sup> )	0.07	0.05	0.07	0.06
	RMSD (cm <sup>3</sup> /cm <sup>3</sup> )	0.07	0.06	0.08	0.06
	$\rho$	0.97	0.97	0.97	0.97
<b>BSh</b>	MD (cm <sup>3</sup> /cm <sup>3</sup> )	0.11	0.07	0.11	0.08
	RMSD (cm <sup>3</sup> /cm <sup>3</sup> )	0.11	0.08	0.12	0.09
	$\rho$	0.93	0.93	0.95	0.95
<b>BWh</b>	MD (cm <sup>3</sup> /cm <sup>3</sup> )	0.08	0.07	0.09	0.07
	RMSD (cm <sup>3</sup> /cm <sup>3</sup> )	0.08	0.07	0.09	0.07
	$\rho$	0.84	0.84	0.85	0.84
<b>Cwa</b>	MD (cm <sup>3</sup> /cm <sup>3</sup> )	0.04	0.02	0.05	0.03
	RMSD (cm <sup>3</sup> /cm <sup>3</sup> )	0.05	0.03	0.06	0.04
	$\rho$	0.93	0.93	0.95	0.95
<b>Cwb</b>	MD (cm <sup>3</sup> /cm <sup>3</sup> )	0.02	0.02	0.03	0.03
	RMSD (cm <sup>3</sup> /cm <sup>3</sup> )	0.03	0.03	0.04	0.04
	$\rho$	0.76	0.77	0.77	0.78

240

241

242

243

244

245

246

247

248

249

250

251

252  
253

**Table S4:** Performance metrics (RMSE, ME, and  $\rho$ ) for soil moisture vs GLEAM (SM: 100 cm).

<b>Climate Zone</b>	<b>Metric</b>	<b>IMDAA-Irr</b>	<b>IMDAA-Rfd</b>	<b>ERA5-Irr</b>	<b>ERA5-Rfd</b>
<b>Am</b>	MD (cm <sup>3</sup> /cm <sup>3</sup> )	-0.04	-0.04	-0.04	-0.04
	RMSD (cm <sup>3</sup> /cm <sup>3</sup> )	0.06	0.06	0.05	0.05
	$\rho$	0.95	0.95	0.95	0.95
<b>Aw</b>	MD (cm <sup>3</sup> /cm <sup>3</sup> )	0.05	0.04	0.05	0.05
	RMSD (cm <sup>3</sup> /cm <sup>3</sup> )	0.05	0.04	0.06	0.05
	$\rho$	0.94	0.94	0.95	0.94
<b>BSh</b>	MD (cm <sup>3</sup> /cm <sup>3</sup> )	0.08	0.06	0.09	0.07
	RMSD (cm <sup>3</sup> /cm <sup>3</sup> )	0.09	0.07	0.09	0.07
	$\rho$	0.92	0.90	0.93	0.91
<b>BWh</b>	MD (cm <sup>3</sup> /cm <sup>3</sup> )	0.10	0.08	0.10	0.09
	RMSD (cm <sup>3</sup> /cm <sup>3</sup> )	0.10	0.09	0.10	0.09
	$\rho$	0.79	0.77	0.80	0.78
<b>Cwa</b>	MD (cm <sup>3</sup> /cm <sup>3</sup> )	0.01	0.00	0.02	0.01
	RMSD (cm <sup>3</sup> /cm <sup>3</sup> )	0.03	0.02	0.03	0.02
	$\rho$	0.92	0.91	0.93	0.92
<b>Cwb</b>	MD (cm <sup>3</sup> /cm <sup>3</sup> )	-0.02	-0.03	-0.02	-0.02
	RMSD (cm <sup>3</sup> /cm <sup>3</sup> )	0.03	0.04	0.03	0.03
	$\rho$	0.63	0.63	0.67	0.68

254  
255  
256  
257  
258  
259  
260  
261  
262  
263  
264

265 **Table S5:** Summary of data used for CLM5 validation.

Variable	Data Source	Data period	Spatial Resolution	Temporal Resolution	Data Source
ET	GLEAM	1980 - 2020	0.25 <sup>0</sup>	Daily	<a href="http://www.gleam.edu">www.gleam.edu</a>
Runoff	GRUN	1980 - 2014	0.5 <sup>0</sup>	Monthly	<a href="#">GRUN: Global Runoff Reconstruction</a>
SM	GLEAM	1980 – 2020	0.25 <sup>0</sup>	Daily	<a href="http://www.gleam.edu">www.gleam.edu</a>
SM	COSMOS	2015 – 2019	3 sites, at 5 cm depth	Daily	<a href="https://cosmos-india.org/">https://cosmos-india.org/</a>
SM	SMAP	2015-2020	~36 km	Daily	<a href="https://appeears.earthdatacloud.nasa.gov/">https://appeears.earthdatacloud.nasa.gov/</a>
SM	GLDAS	1980-2014	0.25 <sup>0</sup>	3-hourly	<a href="https://disc.gsfc.nasa.gov/datasets">https://disc.gsfc.nasa.gov/datasets</a>

266

267

268 **Table S6.** Annual averages of meteorological elements from different meteorological forcing  
 269 datasets for the period of 1980–2020 over India

Variable	IMDAA	ERA5	Difference (IMDAA-ERA5)
Shortwave radiation (W/m <sup>2</sup> )	240.30	217.13	23.17
Downward longwave radiation (W/m <sup>2</sup> )	365.19	364.53	0.66
Air Temperature (K)	295.58	295.50	0.08
Wind speed (m/s)	5.71	5.48	0.23
Relative Humidity (RH: %)	61.70	83.67	-21.97

270

271

272

273

274